Extended Abstracts of the 2018 International Conference on Solid State Devices and Materials, Tokyo, 2018, pp1045-1046

Smartly Designed Tin Oxide Nanoparticles using a Novel Ball Milling Technique Towards High-Performance Planar Perovskite Solar Cells

Mriganka Singh[1], Hong-Cheu Lin[1], Chih-Wei Chu[2], and Gang Li[3]

[1] Department of Materials Science and Engineering,
National Chiao Tung University, Hsinchu 30013, Taiwan (ROC)
[2] Research Center for Applied Sciences,
Academia Sinica, Taipei, 115, Taiwan (ROC)
Phone: +886-02-2787 3183 E-mail: gchu@gate.sinica.edu.tw
[3] Department of Electronic and Information Engineering,
The Hong Kong Polytechnic University, Hung Hom, Kowloon, Hong Kong, China
Phone: +852-2766 7723 E-mail: gang.w.li@polyu.edu.hk

Abstract

Metal oxide transporting layer in organic-inorganic perovskite solar cells (PSCs) have a tremendous improvement in both aspects, first stability and second high power conversion efficiency (PCE), which open a new paradigm for commercialization in near future. Herein we report for the first time a novel home-made ball milling technique for the synthesis of tin oxide (SnO_2) nanoparticles (10~20 nm sizes) fabricated at room temperature, employed as an electron transporting material (ETM) in planar PSCs. A smartly designed ground SnO_2 (G-SnO_2) NPs acts as a mesoporous layer and an additional layer of a SnO_2 layer (C-SnO_2) which is converting from the precursor ($SnCl_2.2H_2O$), acts as compact layer to use for fabrication of high-performance PSCs. A C-SnO_2 layer helps to improve the bonding and interlayer recombination between ETL and absorber layer. We fabricated C-SnO_2, G-SnO_2, and C-SnO_2/G-SnO_2 based PSCs, with champion PCE of 16.28%, 16.35%, and 18.20% respectively, with an active area of 0.04 cm^2.

1. Introduction

In past ten years organic-inorganic hybrid perovskite solar cells (PSCs) reached a higher power conversion efficiency (PCE) from 3.8%[1] to more than 22%[2]. Due to high charge carrier mobilities and tunable band gaps.[3] Basically, PSCs have two kind of device structure conventional (n-i-p)[4] and inverted (p-i-n)[5]. Most commonly used electron transporting materials (ETMs) are titanium dioxide (TiO_2)[6] and tin (IV) oxide (SnO_2)[7]; the hole transporting material is spiro-OMeTAD[8].

In this work, we demonstrated a new approach to prepare the tin oxide (SnO_2) nanoparticles with the help of the ball-milling process to fabricate the planar PSCs with high-performance. A newly way to prepare the SnO_2 involves no rigorous chemical synthesis, it is purely based on physical method. Later, to enhance the charge mobility in the device, we are reporting the combinational electron transporting layer. A compact SnO_2 (C-SnO_2) which is converting from the precursor ($SnCl_2.2H_2O$), act as compact layer and newly ground SnO_2 (G-SnO_2) acts as mesoporous layer. The highest PCE achieved by the combinational ETL (C-SnO_2/G-SnO_2) is 18.2 % with current density, voltage and fill-factor is 21.48 mA cm^{-2}, 1.10 V and 77.04% respectively.

2. Result and discussions

The schematically representation of controlling tin oxide (SnO_2) particle size through physical method shown in Fig. 1(a). In this high-energy wet-milling grinding method, a large clump of SnO_2 undergoes through the physical process (without any rigorous chemical synthesis), only by using zirconia beads and iso-propyl alcohol (IPA) solvent for the ground to achieve a suspension of SnO_2 NPs. Previously our group reported the same strategy to prepare the TiO_2 NPs for bulk heterojunction[9] as well as PSCs[10]. Photograph of without grinding of SnO_2 powder shown in inset of Fig. 1(a). To find out

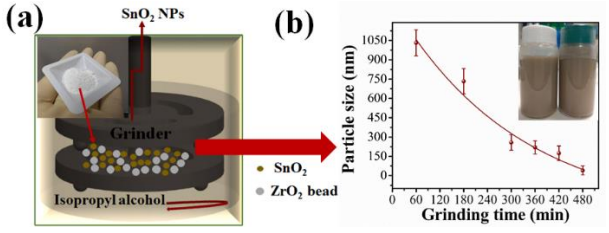

Fig. 1(a) Schematically representation of controlling SnO_2 particle size through physical method, photograph of without grinding of SnO_2 powder in inset of (a), (b) particle size with different grinding time in dynamic light scattering analysis, photograph of SnO_2 solution after the grinding in inset of (b).

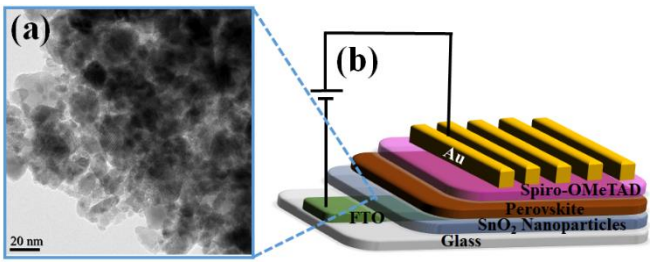

Fig. 2(a) Bright-field TEM image of the ground SnO_2 (G-SnO_2 NPs). (b) Schematic illustration of the device structure: glass/FTO/SnO_2/Perovskite/spiro-OMeTAD/Au.

the actual particle size of ground SnO_2 (G-SnO_2) nanoparticles (NPs), we performed the dynamic light scattering (DLS) measurement and found that G-SnO_2 NPs particle size reduced each hour of grinding time, which is clear from the Fig. 1(b). Inset of Fig. 1(b), photograph shows the evidence of SnO_2 solution after the grinding of G-SnO_2. Transmission electron microscopy (TEM) image of G-SnO_2 NPs shown in the Fig. 2(a). It is clear from bright-field TEM image that the particle size of G-SnO_2 NPs around 10 to 20 nm. The device architecture [glass/FTO/SnO_2/Perovskite/spiro-OMeTAD/Au] for planar PSCs shown in the Fig. 2(b). *J-V* curve of the best performing perovskite based solar cell using different ETL [C-SnO_2 or G-SnO_2 (or C-SnO_2/G-SnO_2)] layer measured under reverse voltage scans shown in Fig. 3. All the device performance of the best cell of different ETL layer summarized in the table, which is shown in inset of Fig. 3.

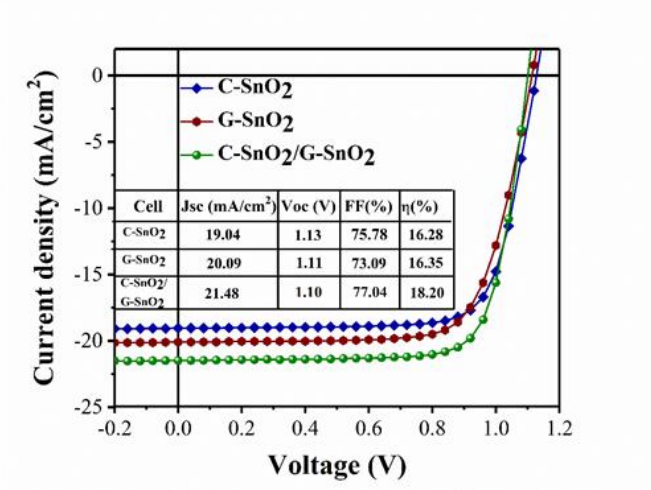

Fig. 3 *J-V* curve of the best performing perovskite based solar cell using different ETL [C-SnO_2 or G-SnO_2 (or C-SnO_2/G-SnO_2)] layer measured under reverse voltage scans.

The morphology studies of G-SnO_2 on the top of FTO and C-SnO_2 are revealing from scanning electron microscopy (SEM) images shown in the Fig. 4(a), and Fig. 4(b). It seems the FTO/C-SnO_2/G-SnO_2 have better surface coverage than the pristine G-SnO_2, is the main reason for better performance for C-SnO_2/G-SnO_2 ETLs.

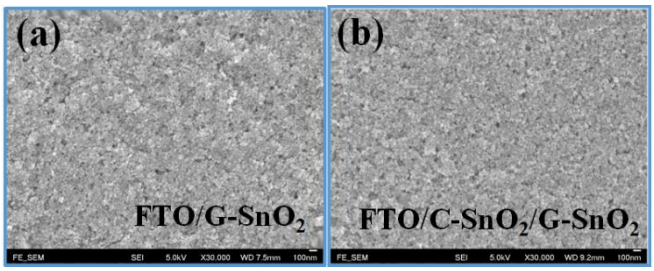

Fig. 4 SEM surface morphology images of (a) FTO/G-SnO_2, and (b) FTO/C-SnO_2/G-SnO_2.

3. Conclusions

In conclusion, we have prepared the G-SnO_2 NPs by a ball-milling method for planar PSCs. TEM and DLS revealed the average particle size of the G-SnO_2 NPs ~ 10-20 nm. PSCs associated with two ETLs shows the best PCE is 18.2 %.

Acknowledgements

Dr. Chu thanks the Ministry of Science and Technology (MOST) of Taiwan (104-2221-E-001-014-MY3) and the Career Development Award of Academia Sinica, Taiwan (103-CDA-M01), for financial support.

References

[1] A. Kojima, K. Teshima, Y. Shirai and T. Miyasaka, *J. Am. Chem. Soc.*, **17** (2009), 6050-6051.

[2] National Renewable Energy Laboratory (NREL), 2017, https://www.nrel.gov/pv/assets/images/efficiency-chart.png, (accessed: November 2017.

[3] Y. Wang, Y. Zhang, P. Zhang and W. Zhang, Phys. Chem. Chem. Phys., **17** (2015), 11516–11520.

[4] W. S. Yang, J. H. Noh, N. J. Jeon, Y. C. Kim, S. Ryu, J. Seo and S. I. Seok, *Science*, **348** (2015), 1234-1237.

[5] I. J. Park, M. A. Park, D. H. Kim, G. D. Park, B. J. Kim, H. J. Son, M. J. Ko, D.-K. Lee, T. Park and H. Shin, *J. Phys. Chem. C*, **119** (2015), 27285-27290.

[6] H. Tan, A. Jain, O. Voznyy, X. Lan, F. P. G. de Arquer, J. Z. Fan, R. Quintero-Bermudez, M. Yuan, B. Zhang and Y. Zhao, *Science*, **355** (2017), 722-726.

[7] G. Yang, H. Lei, H. Tao, X. Zheng, J. Ma, Q. Liu, W. Ke, Z. Chen, L. Xiong and P. Qin, *Small*, **13** (2017), 2.

[8] H. Li, W. Shi, W. Huang, E.-P. Yao, J. Han, Z. Chen, S. Liu, Y. Shen, M. Wang and Y. Yang, *Nano Lett.*, **17** (2017), 2328-2335.

[9] J. H. Huang, M. A. Ibrahem and C. W. Chu, *Progress in Photovoltaics: Research and Applications*, **23** (2015), 1017-1024.

[10] M. Singh, C. H. Chiang, K. M. Boopathi, C. Hanmandlu, G. Li, C. G. Wu, H. C. Lin and C. W. Chu, *J. Mater. Chem. A,* **6** (2018), 7114-7122.